

Crossover from incoherent-metal to Fermi-liquid behavior in CuV_2S_4 : Transport and magnetic properties upon substituting Zn for Cu

I. Naik, C. S. Yadav, and A. K. Rastogi

School of Physical Sciences, Jawaharlal Nehru University, New Delhi-67, India

(Received 28 January 2006; revised manuscript received 3 October 2006; published 21 March 2007)

We present the results of the measurements of electrical conductivity, thermopower, and magnetization of the Sulfospinel CuV_2S_4 and its Zn-substituted compounds between 2 and 600 K. We confirm the existence of two electronic transitions at around 90 and 54 K in the pure phase. The sharpness of the transition at 90 K is reduced by Zn substitution. Above 90 K the dependence of resistivity on temperature (T) in all the compounds is of the form $\rho_0 + A/T + BT$ —with anomalously large values of ρ_0 and B . In the same temperature range the thermopower decreases linearly with increasing temperature and becomes negative above 500 K. These results regarding resistivity and thermopower are quite unusual for a normal metal. But they are reminiscent of the in-plane transport properties of high- T_c -cuprate superconductors and suggest highly incoherent dynamical behavior of current carriers in our compounds. These high temperature properties are also consistent with the presence of a pseudogaplike feature at the Fermi level—as has been seen earlier in the photoemission measurements in these compounds. Below 50 K the electronic properties are qualitatively different and can be understood in terms of a weakly correlated and exchange enhanced Fermi liquid. This inference is based partially on our analysis of the magnetization data at 2 K and high field (up to 7 T) in terms of the Stoner model of itinerant electrons. This analysis shows that the exchange splitting of the d bands is substantial and dominates the e - e repulsion—thus inhibiting a superconducting transition.

DOI: [10.1103/PhysRevB.75.115122](https://doi.org/10.1103/PhysRevB.75.115122)

PACS number(s): 71.27.+a, 75.30.Fv, 71.45.Lr, 72.80.Ga

INTRODUCTION

The sulfospinels of Cu (CuM_2S_4 with $M = \text{Ti, Zr, Hf, V, Cr, Co, Rh, and Ir}$) show metallic conduction and Pauli paramagnetism. The only exception is the Cr sulfospinel which has a relatively high ferromagnetic transition at 420 K.^{1,2} There has been considerable interest in these compounds because of the rich variety of phase transitions at low temperatures. CuRh_2S_4 becomes superconducting below 4.7 K and shows superconductor-insulator transition at high pressure.³ In CuIr_2S_4 a metal-insulator transition is observed at 230 K [Ref. 4(a)] due to charge ordering—which results in bicapped hexagonal rings of Ir_8^{3+} and Ir_8^{4+} octamers in a spinel lattice.^{4(b)}

CuV_2S_4 shows sharp anomalies in electrical and magnetic properties around 90 and 50 K. The transitions here are attributed to a charge density wave (CDW) instability which is rare in a cubic compound.⁵ It is an unusual behavior because CuV_2S_4 has the largest magnetic susceptibility and electronic specific heat among all the members of the family and exchange energy considerations should favor spin density modulation (SDW) of electronic charges—as first proposed by Overhauser⁶ for the Cr metal.

At 90 K a lattice distortion and the associated gapping of the Fermi surface is observed in the magnetic susceptibility of pure CuV_2S_4 (as expected for CDW/SDW instability). At 54 K another transition with a sharp increase in the magnetic susceptibility on cooling is found. Interestingly the phase below 54 K shows remarkably improved metallic properties—as seen in the temperature dependence of conductivity as well as thermopower. However, there is no superconductivity or magnetic order down to 60 mK.

Detailed band structure calculations as well as x-ray photoemission measurements show that the diamagnetic Cu^{+1} in

CuV_2S_4 does not contribute to the electronic properties and also that the high density of states at the Fermi level is largely due to narrow bands from $3d$ orbitals of vanadium. Lu *et al.*⁷ find a relatively large value of 3.6 orbitals/(eV f.u.) for the density of states (DOS) at the Fermi level. The exchange and correlation effects are quite significant in CuV_2S_4 and both the magnetic susceptibility (χ) and the electronic specific heat coefficient (γ) are enhanced by a factor of about 10 above the value expected from the DOS.

Photoemission experiments of Matsuno *et al.*⁸ on CuV_2S_4 and CuTi_2S_4 suggest that correlations have significantly smaller effects on the electronic band structure in these sulfospinels than in the case of the oxides of vanadium. Nevertheless, these experiments (which were performed at temperatures below 350 K) revealed the existence of some anomalies at the Fermi level in CuV_2S_4 . These are (a) as the temperature is reduced progressively the height of the local minimum of the DOS function at the Fermi level keeps decreasing through the transfer of spectral weight to lower energies and (b) the energy scale of the pseudogap is found to be anomalously large (~ 100 meV) and remains practically independent of temperature. The presence of the pseudogap up to fairly high temperatures in CuV_2S_4 has been attributed to correlated fluctuations of charges and spins along the nesting vectors $q \sim 1/4 [110]$ of the V chains.⁸

As shown in Fig. 1 there are six $\langle 110 \rangle$ directions in the cubic lattice for the linear chains of V atoms occupying the B sites of spinel structure. In addition, these sites also form a topologically frustrated pyrochlore-type lattice of corner sharing tetrahedra. The topological frustration of the B -site network as well as the contributions of nearly one-dimensional bands arising out of the linear chains have negative consequences on the long range ordering of charges and spins at low temperatures. These are important structural fea-

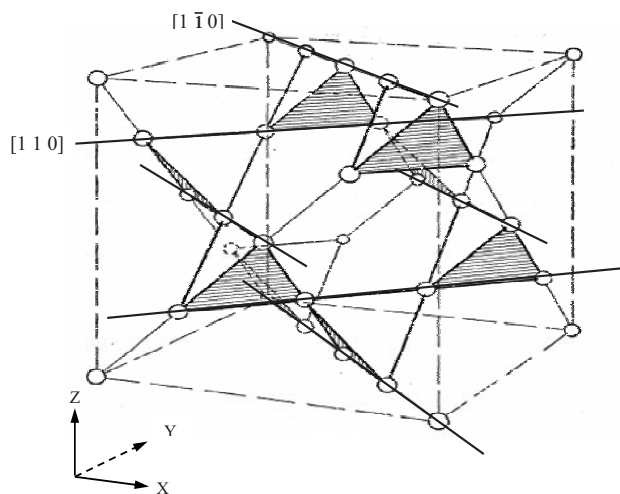


FIG. 1. The octahedral B sites of a spinel structure of CuV_2S_4 forming corner sharing V tetrahedra and the linear chains running along $\langle 110 \rangle$ directions.

tures and may well explain the high temperature transport and magnetic properties as being due to strong fluctuations of charge/spin ordering in CuV_2S_4 .

CuV_2S_4 has been studied extensively for its unusual electronic phase transitions.^{2,5,7,9} The dependence of resistivity on temperature around the transition at 90 K is quite sensitive to the presence of impurities. In many earlier studies the sharp drop on cooling across the transition temperature was not observed and, contrary to the results from later studies on pure phases, resistance continued to rise until the 54 K transition. In a recent study it was shown that the 90 K anomaly is also absent in the resistivity of the single crystals grown by TeCl_4 vapors.¹⁰ Crystals obtained with I_2 vapor, however, gave very sharp changes at 90 and 54 K in the electrical, magnetic, and thermal properties.¹¹ The small specific heat observed by the temperature sweep method indicated that the 90 K transition is intermediate between first and second order and the 54 K transition is of first order with a hysteresis.¹¹

The physical origin and the nature of the lattice distortion in CuV_2S_4 at 90 K are not very clear. Fleming *et al.*⁵ proposed the first interpretation in terms of the onset of CDW instability at 90 K. The x-ray diffraction (XRD) studies showed an incommensurate distortion of the cubic lattice at 90 K, with a wave vector $\vec{q} = (1/4 - \delta) [110]$. On cooling down to 75 K δ continuously decreases to zero and the distortion becomes commensurate. On cooling further another incommensurate structure $\vec{q} \approx 1/3 [110]$ was found at 50 K. However, a subsequent study using electron-diffraction gave a deformation modulated structure—resulting in a cubic to orthorhombic transformation at 90 K.¹² The incommensurability in this study was found to be related to the quasiperiodically stacked antiphase boundaries of the differently oriented domains below the transition. Another XRD study by Yoshikawa *et al.*¹³ reported a cubic-tetragonal transition at 90 K. This was, however, found to be absent by Matsuno *et al.*⁸ in TeCl_4 -grown single crystals.

We have substituted Cu by Zn in CuV_2S_4 and studied magnetic and transport properties in detail on sintered pellets

between 2 and 600 K. Our pellets of pure phase show all the expected features, including sharp anomalies, in the electronic properties at both the transitions—as reported for single crystals grown by I_2 -vapor transport. Thermopower measurements have not been performed earlier on the compounds studied here. Results on conductivity, thermopower, and magnetization are reported in separate sections. This is followed by a discussion of our main results.

EXPERIMENT

Sample preparation

The first step in the preparation of the samples is a direct reaction of the pure elements in sealed quartz tubes at 800 °C. This is followed by grinding and pelletization in a dry box. Finally the samples are sintered at 800 °C for seven days. XRD patterns showed a well-crystallized cubic phase with $a = 9.808 \text{ \AA}$ which is the same as reported earlier. For Zn-substituted compounds repeated grinding and sintering was needed to eliminate ZnS impurities. The reannealed samples will be designated by suffixing -R. We were able to prepare homogeneous cubic phases with the extent of substitution of Cu by Zn only up to 20%. The cubic lattice parameter increases slightly with substitution and reaches the value of 9.816 Å for 20% Zn.

Measurements

All the measurements reported here were performed on pellets. Resistance was measured using the van der Pauw method¹⁴ on circular pellets and using silver paste for the contacts. Absolute thermopower was measured with respect to Cu by reversing the temperature gradient along a rectangular pellet at different temperatures and correcting for the thermopower of Cu. Magnetic measurements were done with a superconducting quantum interference device magnetometer with temperatures down to 2 K and the field strength up to 7 T.

ELECTRICAL CONDUCTIVITY

Resistivity data for two samples of CuV_2S_4 (annealed differently, pure and pure-R) in the temperature range of 2 to 600 K are shown in Fig. 2. The two transitional anomalies seen in this figure are very similar to those reported for I_2 -grown single crystals.^{5,11} On cooling below room temperature, a broad minimum is found at around 120 K. This is followed by a cusp like transition at 90 K. At 54 K there is a hysteretic transition and a downward jump in the resistivity can be clearly seen on cooling sample 2 (pure-R) which is annealed for longer duration. The resistance ratio $\rho_{300 \text{ K}} / \rho_{2 \text{ K}}$ equals 12 for this sample and this is greater than the value of 8.5 reported by Sekine *et al.*¹¹ in I_2 -grown single crystals.

At room temperature the resistivity of both the samples is $\sim 400 \mu\Omega \text{ cm}$. This is greater than the value of $290 \mu\Omega \text{ cm}$ obtained for I_2 -grown single crystals but is significantly lower than what is found for TeCl_4 -grown crystals ($600 \mu\Omega \text{ cm}$).^{9,10} This clearly indicates that the observed resistivity is intrinsic to CuV_2S_4 and is not significantly af-

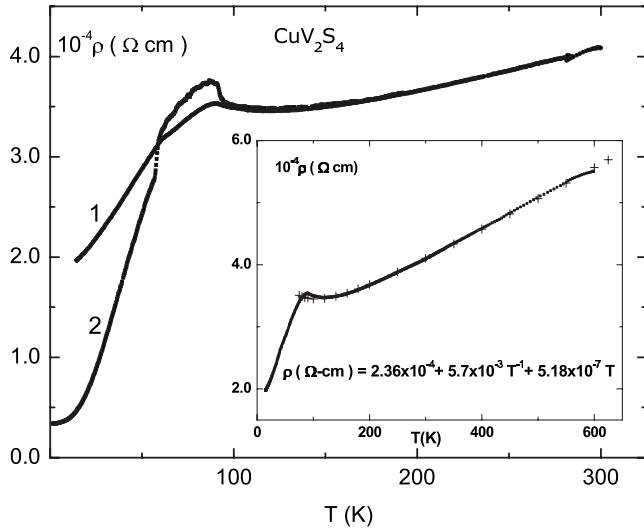


FIG. 2. The resistivity plots of two differently annealed samples 1,2 of CuV_2S_4 showing transition at 90 and 54 K. The anomalies at the transitions become stronger after extended annealing for sample 2. The points marked by + in the inset are the fit to resistivity $\rho(T) = \rho_0 + AT^{-1} + BT$ between 90–600 K.

ected by the intergrain coupling in a polycrystalline pellet.

The overall behavior of the high temperature resistivity remains unaffected in Zn-substituted compounds and all of them show a resistance-minimum around 120 K. However, the cusp at 90 K is suppressed even when only 5% of Cu is substituted—as can be seen in Fig. 3. And for all the Zn-substituted compounds the resistance continues to increase on cooling through 90 K. This is followed by a broad maximum at ~ 40 K. Thus the data on resistivity does not contain any signature of the transition at around 50 K. However, the thermopower and magnetic susceptibility measurements show that this transition persists in Zn—substituted compounds.

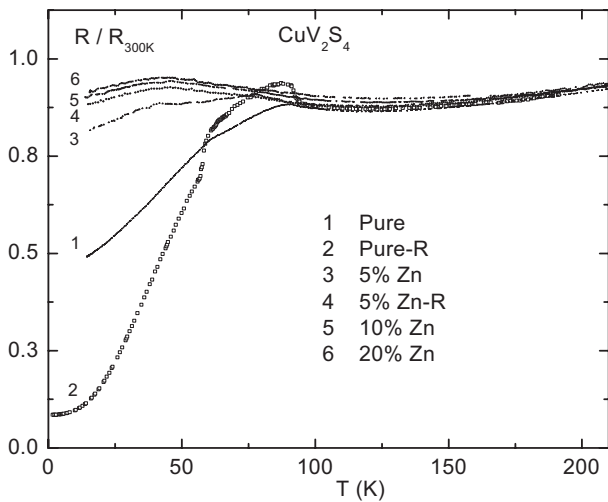


FIG. 3. The normalized resistivity plots of $\text{Cu}_{1-x}\text{Zn}_x\text{V}_2\text{S}_4$ compounds showing the suppression of the cusp at 90 K transition and a broad maximum around 40 K on Zn substitution of Cu. The suffix-R is for the reannealed samples.

For both pure and Zn-substituted samples the dependence of resistivity (ρ) on temperature (T) can be described rather accurately by the following relation:

$$\rho = \rho_0 + \frac{A}{T} + BT. \quad (1)$$

For the pure phase the quality of the fit between 90 and 600 K can be seen from the inset of Fig. 2. Best fit values of the parameters are $\rho_0 = 230 \mu\Omega \text{ cm}$, $A = 5.7 \text{ m}\Omega \text{ cm K}$, and $B = 0.52 \mu\Omega \text{ cm K}^{-1}$. Hence, in addition to a rather high value of ρ_0 , there is an anomalous $1/T$ component of the high temperatures resistivity of these compounds. With increasing Zn substitution both ρ_0 and A increase monotonically and assume the values of $300 \mu\Omega \text{ cm}$ and $7.0 \text{ m}\Omega \text{ cm K}$, respectively, for 20% Zn. For every compound the value of B , the coefficient of the linear term, is too large to be understood purely in terms of electron-phonon (e -ph) scattering. We believe that it is more likely due to the incoherent scattering of electrons from the marginally localized spin and charge fluctuations at high temperatures. This e - e scattering is the cause of the pseudogap observed in the DOS function,⁸ as had been widely discussed in the case of the normal state of the cuprate superconductors.¹⁹

The strong reduction of resistivity in CuV_2S_4 below 90 K clearly suggests an electronic phase transition and the remarkable suppression of incoherent scattering of carriers in the low temperature ordered phase. In Zn-substituted compounds (or in crystals grown in TeCl_4 vapor¹⁰) the long range order is destroyed by the lattice defects. As a result the resistance is primarily due to ionic scattering and its value remains high at low temperatures.

Crandles *et al.*¹⁰ have analyzed the conductivity and optical reflectivity data for single crystals—assuming that conduction is isotropic and $m^* = m_e$. In their analysis the observed free carrier absorption could be fitted with Drude's relation and the best fit values of the plasma frequency ω_p and the scattering rate Γ were found to be equal to $3.7 \times 10^{15} \text{ rad sec}^{-1}$ and $5.1 \times 10^{14} \text{ sec}^{-1}$, respectively. This leads to a value of $5 \times 10^{21} \text{ cm}^{-3}$ for the density of electrons and it was considered to be consistent with the observed Hall coefficient at room temperature. The observed resistivity of $400 \mu\Omega \text{ cm}$ would then give a mean free path $\lambda (= v_F \tau)$ of 12 Å. Thus, although the scattering length is comparable to the dimensions of the cubic cell, the conductivity is well within the metallic side—since the value of the localization parameter ($k_F \lambda \approx 6$) is greater than the Ioffe-Regel limit of π . Hence the semiclassical Boltzmann formulation for the dynamics of the electrons seems to be justified.

However, the above analysis ignores the strong effects of scattering which actually give rise to the minimum in the plot of resistance versus temperature and the anomalously large value of the coefficient of the linear term of the fitting function for our data. In view of these in the following we will analyze the conductivity data after taking account of strong scattering effects.

In the case of strong scattering ($k\lambda \sim \pi$ or $\Delta k/k \sim 1$) k is not a good quantum number and large changes in the density of electronic states are expected. Therefore, the semiclassical

Boltzmann formulation for the transport coefficients is no longer applicable. For the Hall coefficient the sign is related to the details of the successive scattering events and its value is expected to be much less than what is predicted by the free electron theory.¹⁵ This is consistent with the measurements of Horny *et al.*¹⁶ Moreover, in the case of spin dependent scattering, the Hall coefficient may have an extraordinary component and it cannot be used for estimating carrier density.

For arbitrary values of $k_F\lambda$ we can use the Kubo-Greenwood formula for the electrical conductivity as given by the following expression:

$$\sigma(\omega) = \frac{S_F e^2 \lambda}{12 \pi^3 \hbar} \frac{1}{1 + \omega^2 \tau^2}. \quad (2)$$

Here S_F is the area of the Fermi surface, τ is the relaxation time, and λ is the mean distance over which the phase of the wave function gets randomized due to scattering events.¹⁵ The above formula does not contain band mass explicitly. To account for the effect of multiple scattering and the consequent modification of the density of states at the Fermi level [$N(\epsilon_F)$], Mott¹⁵ has introduced a factor g given by $N(\epsilon_F)/N(\epsilon_F)_{\text{band}}$. Using this, the expression for the dc conductivity becomes

$$\sigma = \frac{S_F e^2 \lambda g^2}{12 \pi^2 \hbar}. \quad (3)$$

For our analysis we will take the value of g to be unity. Also the band structure of CuV_2S_4 is approximated to be isotropic—as a result of which

$$N(\epsilon_F) = \frac{S_F}{4 \pi^3 \hbar v_F}. \quad (4)$$

Equation (3) then reduces to

$$\sigma = \frac{N(\epsilon_F) e^2 \lambda^2}{3 \tau}. \quad (5)$$

Using the value of $N(\epsilon_F) = 2.85 \times 10^{22}$ states $\text{eV}^{-1} \text{cm}^{-3}$ (taken from Ref. 7), $\tau = 2 \times 10^{-15}$ sec (obtained from the optical conductivity data¹⁰), and the value of conductivity at room temperature, we obtain a value of 5.7 \AA for λ . The value of k_F is obtained by taking three electrons per formula unit. This finally leads to the values of $k_F\lambda$ and m^* ($= \hbar k_F / v_F$) equal to 5.1 and $3.6 m_e$, respectively. There is nothing unusual about these values and it once again indicates that the localization parameter is well above the Ioffe-Regal limit. Using three electrons per formula unit, we obtain 1.25 eV for the value of ϵ_F . This compares well with the value of approximately 1 eV calculated by Lu and Klin *et al.*⁷ Thus we see that CuV_2S_4 is well within the metallic regime and the high value of its resistivity can be broadly understood within the Kubo-Greenwood formalism—although the inclusion of electron-electron interactions will significantly alter this simple independent electron picture.

The peculiarity of CuV_2S_4 is that its resistivity is large and keeps increasing with temperature even at 600 K. Moreover, the large value of the scattering rate for the carriers

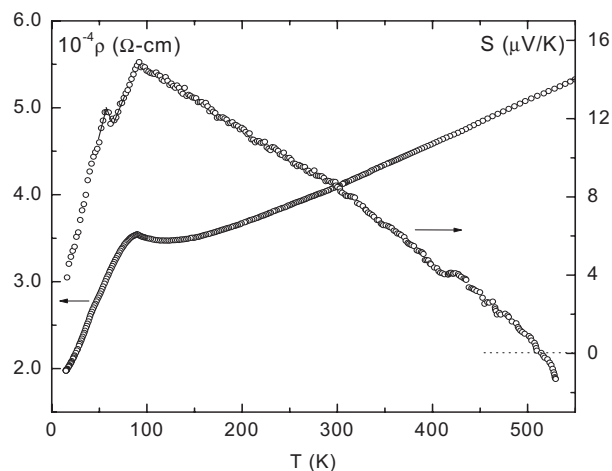


FIG. 4. The behavior of the resistivity and Seebeck coefficient of CuV_2S_4 between 15 and 600 K, showing both transitions at low temperatures. Above 90 K the Seebeck coefficient reduces linearly and becomes negative above 500 K.

($1/\tau = 5 \times 10^{14}$ sec) would imply an energy uncertainty of 0.33 eV—which is comparable to the width of the conduction bands. In this situation scattering will cause interband transitions and would invalidate the semiclassical model as well as the quasiparticle picture in a Fermi liquid. For a proper understanding of the transport properties a detailed study of the nature of pseudogap features (observed in the photoemission study⁸) and the effect of inelastic scattering is therefore required.

We remark that the electronic properties of CuV_2S_4 are qualitatively different from those of highly correlated electron systems (V_2O_3 and NiS, etc). For the latter case there is strong dependence on the extent of doping and electronic correlations lead to metal-insulator transitions. On the metallic side their properties can be understood in terms of Hubbard bands with small overlap. This results in a small effective density of carriers ($\sim 10^{-6}$ per metal atom) in the doubly occupied levels.¹⁵ This is in contrast to the case of CuV_2S_4 in which there is no effect of doping and the density of conduction electrons (~ 1 per V atom) is very large. But, due to strong scattering from charge/spin fluctuations, the electronic properties at high temperatures are qualitatively different from those of a normal metal.

Interestingly, the dependence of resistivity on temperature [$\rho(T) = A/T + BT$] is strikingly similar to that for the c -axis resistivity of high quality single crystals of cuprate superconductors (HTS). In the latter case the normal state conductivity is above Mott's minimum value and displays the same temperature dependence very closely over a large range of temperatures.¹⁷⁻¹⁹ This anomalous behavior has been discussed extensively in terms of the theory of non-Fermi liquids which incorporates the effects of strong inelastic e - e scattering due to charge and spin fluctuations.²⁰

THERMOPOWER

In Fig. 4 we plot the Seebeck coefficient (S) and the resistivity (ρ) of the pure phase as a function of temperature.

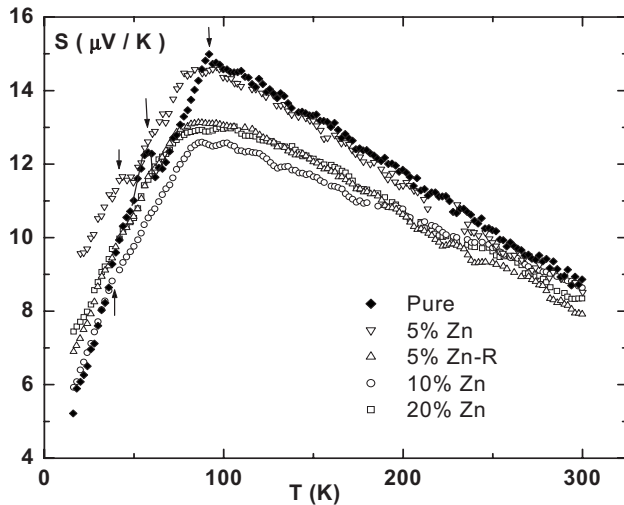


FIG. 5. The temperature dependence of the Seebeck coefficient of pure and $\text{Cu}_{1-x}\text{Zn}_x\text{V}_2\text{S}_4$ showing a maximum around 90 K.

The anomalies associated with the transitions at 54 and 90 K can also be seen in the thermoelectric properties. The temperature dependence of S at low temperatures is metal-like with a linear rise up to 54 K. At 54 K a small jump can be noticed in S and this feature is in common with the data for resistivity and magnetic susceptibility. At higher temperatures the behavior of the Seebeck coefficient is quite different from that of a simple metal. Beyond the sharp cusp at 90 K we find a nearly linear drop in the thermopower with temperature. As can be seen in Fig. 5 this behavior is hardly affected by Zn substitution. This relative insensitivity of the value of S to the presence of ionic defects suggests that the enhancement of thermopower with decrease in temperature cannot be explained in terms of phonon drag. Moreover, in view of strong incoherent scatterings and its bootstrapping effect on the phonons, a coherent drag of electrons by the phonons is not likely in the pure phase.

The appearance of a peak in the $S(T)$ function (seen here at ~ 90 K) is quite common for transition metals and their compounds. It is also seen in underdoped high- T_c materials. In the latter case Hildebrand *et al.*²⁰ explained this feature in terms of electronic excitations across the pseudogap. This pseudogap arises out of short range antiferromagnetic correlations. In our case a similar mechanism may be responsible for the resistance minimum at 120 K and also the significant reduction in magnetic susceptibility on cooling from high temperatures.

MAGNETIC PROPERTIES

The magnetization data for pure CuV_2S_4 and the Zn-substituted compounds, measured in the 1 kOe field from 2 to 300 K, are shown in Figs. 6 and 7, respectively. Previously, DiSalvo *et al.*² reported the results of magnetic susceptibility (χ) measurements for this compound for temperatures up to 700 K. They had observed the anomalies seen in our data around the two transitions at 54 and 90 K (Fig. 6). But, in addition, they also found a broad maximum at 400 K.

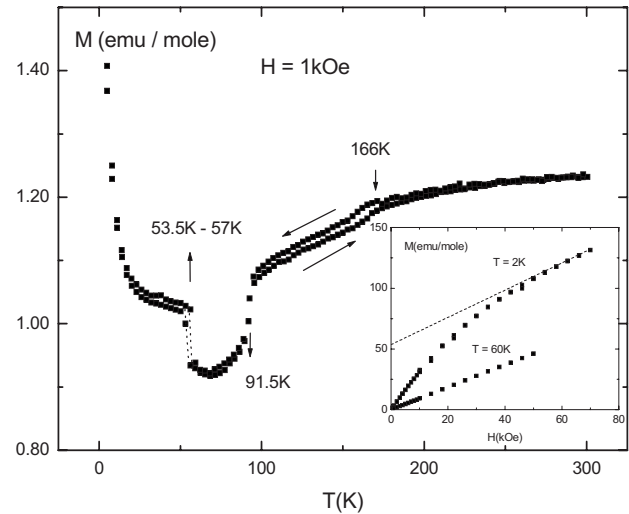


FIG. 6. The temperature dependence of the magnetization of CuV_2S_4 measured in a 1 kOe field. The precursor effects of the 90 K transition can be seen as a rapid drop of the magnetization starting from 166 K. At 54 K transition magnetization jumps up on cooling with a temperature hysteresis. In the inset we show the high field magnetization at 2 and 60 K.

At the 90 K transition the magnetic susceptibility shows significant reduction on cooling. However, our measurements also show a significant precursor effect of this transition. This effect starts in the vicinity of 170 K where a steeper reduction of χ with cooling can be clearly seen in Fig. 6. For the transition around 54 K an upward jump on cooling and associated hysteresis is visible. Below this we find a Curie-like tail ($\chi_c \sim 1/T$)—very similar to that reported by previous workers.^{2,5,9,10,13}

For the Zn-substituted compounds the value of χ depends on the concentration of Zn. For the higher concentrations χ depends on the annealing history of the specimen. The case of (nominal) 20% Zn concentration is presented in Fig. 7, as

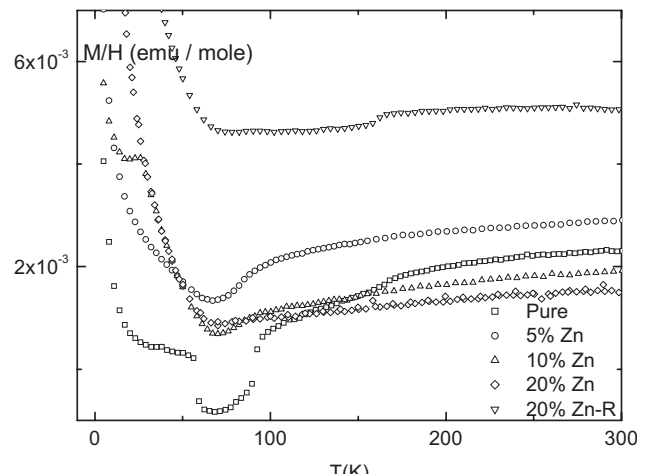


FIG. 7. Magnetic susceptibility $\chi = M/H$ of $\text{Cu}_{1-x}\text{Zn}_x\text{V}_2\text{S}_4$ measured at 1 kOe field. We also show a large increase in the susceptibility of the 20% Zn-R sample after annealing it a second time. A Curie-like increase in χ can be seen on cooling below 60 K for all the samples.

an example of this increased sensitivity. It can be seen that the value of χ increases substantially on repeating the measurement after annealing it for the second time. In the figure, however, apart from this sensitivity, we notice that the temperature dependence of χ is not qualitatively affected for up to 10% of Zn substitution. The decrease in χ on cooling, from the room temperature down to 90 K, becomes progressively less with the increase in Zn concentration. In addition all of them show a rapidly rising (Curie-like) χ at lower temperatures.

Low temperature magnetic properties

Previous workers have discussed the origin of a Curie-like contribution χ_c observed in their low temperature measurements. Disalvo *et al.*² investigated the effect of composition on the magnetic properties of a nominally pure phase and concluded that this contribution is due to some unidentified impurity phase. On the other hand Crandles *et al.*¹⁰ analyzed the high field magnetization data for CuV_2S_4 from several sources and concluded that the Curie-like contribution owes its origin to the small number of paramagnetic centers ($\sim 0.05\%$) which are formed in these systems. These centers interact with the conduction electrons to create large magnetic moments ($\sim 8.5\mu_B$) at low temperatures—the mechanism being the same as in the case of iron atoms in an exchange enhanced metal like palladium. In the following we examine the applicability of this latter interpretation to our data.

Our data for the magnetization as a function of the field were taken at 2 and 60 K and are shown in the inset of Fig. 6. The impurity contribution to the magnetization $M_{\text{im}}(H)$ at 2 K was obtained after subtracting the Pauli component from the total magnetization. Here we assume that the Curie-like contribution from the impurities is entirely absent from the $M(H)$ data at 60 K. The $M_{\text{im}}(H)$ function thus found displays saturation at higher fields and can be fitted to a Brillouin function $B_J(\mu H/k_B T)$ to obtain the value of the magnetic moment μ ($=gJ\mu_B$) on the individual centers. In Fig. 8 we show such fits for two values of J ($=1/2$ and 1) for the data with CuV_2S_4 . Clearly the fit is much closer for $J=1$. Thus we find a normal magnitude of $2\mu_B$ —in sharp contrast to the rather high value of $8.5\mu_B$ found by Crandles *et al.*¹⁰ From the saturated value (σ_s) of magnetization (63 emu mole) the number of localized centers is estimated to be about 0.5% of the number of CuV_2S_4 molecules. A similar analysis was also carried out for the 20% Zn compound. In this case the high field susceptibility at 2 K has the much larger value of 1.8×10^{-3} emu mole $^{-1}$ and the $M_{\text{im}}(H)$ function saturates to $\sigma_s = 24$ emu mole $^{-1}$. As shown in Fig. 8, the best fit to the Brillouin function is obtained for $J=3$. The number of the localized moments in this case (0.07% of CuV_2S_4 molecules) is considerably less than in the pure phase.

Thus we see that our data on pure CuV_2S_4 do not give such large moments on the localizing centers as previously reported by Crandles *et al.*¹⁰ However, we find that the moments are substantially larger and the density is significantly lower in the 20% Zn compounds as compared to the pure CuV_2S_4 . This is contrary to the expectation of an increase in

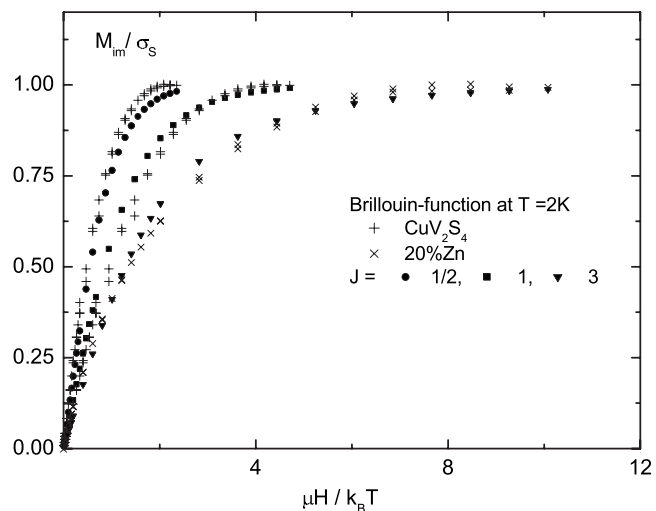


FIG. 8. The contribution of the localized moments to the magnetization at 2 K is fitted to the Brillouin function for different values of J for data of CuV_2S_4 (+) and the 20% Zn substituted sample (\times). See text for the details.

the number of localizing centers when lattice defects are present. In our view the above analysis of the low temperature magnetic properties in terms of impurity centers is not satisfactory. The physical picture involved may itself be wrong—especially for the pure phase. It is generally agreed that the magnetic susceptibility of CuV_2S_4 is substantially enhanced by exchange interactions. In the Stoner-Wohlfarth theory of itinerant electron magnetism a nonlinear $M(H)$, as found here at 2 K, is expected in such cases. In the following we will analyze our data using the predictions of the Stoner-Wohlfarth theory and show that the parameters obtained are quite reasonable and are consistent with the values measured for various other physical properties.

Stoner-Wohlfarth model

In the Stoner model the exchange enhancement factor (S) of the susceptibility is given as $S = 1/[1 - N(\epsilon_F)I_{\text{eff}}]$. Here $N(\epsilon_F)$ is the calculated DOS (per eV–metal-atom-spin) and I_{eff} is the effective Coulomb interaction energy between electron pairs. For our compound CuV_2S_4 the values of the susceptibility χ (0.97×10^{-3} emu mole $^{-1}$) and $N(\epsilon_F)$ [0.9 states/(eV V atom spin)] give 8.5 and 1 eV for S and I_{eff} , respectively.

In the case of itinerant electrons the magnetism is due to the splitting of the conduction band into up and down spin bands by an exchange energy ΔE . The value of ΔE depends on the number of electrons (n) per metal atom, the effective Coulomb interaction energy I_{eff} between electron pairs, and the relative magnetization $\zeta_0 = M(0,0)/nN\mu_B$ of the exchange split band at $H=0$ and $T=0$ and is given by the following relation:²¹

$$\Delta E = nI_{\text{eff}}\zeta_0. \quad (6)$$

Here $M(H, T)$ is the magnetization per mole at temperature T and magnetic field H . N is the Avogadro number. For the

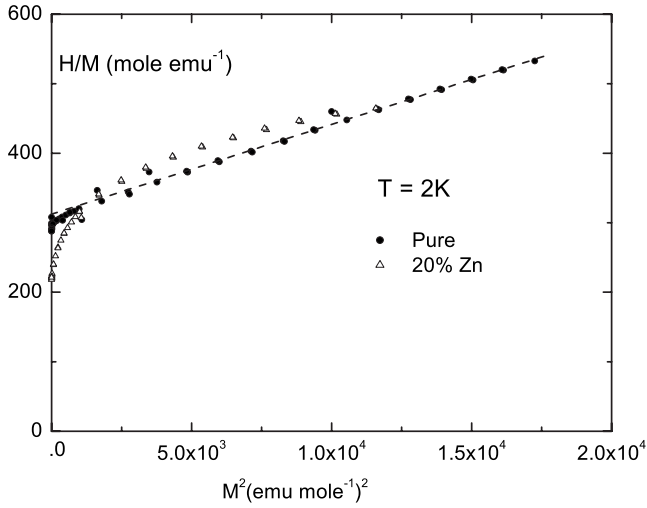


FIG. 9. Arrott plots for the magnetization of the pure CuV_2S_4 and 20% Zn samples at 2 K. A straight line plot, following the relation (7), suggests the absence of localized moments due to impurities in our pure phase.

weakly magnetic systems that we are dealing with the relative magnetization $\zeta [=M(H, T)/nN\mu_B]$ in high fields is much less than unity. Under these conditions the Stoner relations (describing the magnetization as a function of the applied field H and temperature T) can be expanded in powers of T/T_F^* (here the parameter T_F^* is the effective degeneracy temperature of the itinerant electrons and is related to energy derivatives of the density of states at the Fermi energy). By limiting the expansion to the second order we obtain a cubic equation for $\zeta(H, T)$. We can write this in the following form (originally known as the Arrott relation²² applicable to the weak itinerant electron magnet):

$$\frac{H}{M(H, T)} = \frac{M^2(H, T)}{S\chi_{00}M^2(0, 0)} + \frac{1}{S\chi_{00}} \left(\frac{S^{1/2}T}{T_F} \right)^2. \quad (7)$$

$S\chi_{00} = 2NN(\epsilon_F)\mu_B^2/[1 - N(\epsilon_F)I_{\text{eff}}]$ is the exchange-enhanced susceptibility at $H=0$ and $T=0$.

In Fig. 9 we show the plot of H/M versus M^2 for our magnetization data (measured at 2 K from 0 to 7 T fields) for the pure CuV_2S_4 and 20% Zn samples. We can clearly see that the plot for the pure phase is a straight line—as expected from the relation (7). This suggests that the magnetization is homogenous and there are no localized moments in pure CuV_2S_4 . On the other hand, we find a downward curvature in the plot for the 20% Zn sample. This is not unexpected in the theory of itinerant electron magnetism and is explained as being due to the inhomogeneous nature of magnetization of the specimen which is caused by the localized spin fluctuations.²³

For the pure CuV_2S_4 we can find the relative magnetization ζ_0 and can estimate the value of the exchange splitting of the conduction band from the slope of the H/M versus M^2 curve. Using this value of ζ_0 (0.016/electron) and the known value of n (1.5 electrons per V atoms) the value of the exchange splitting ΔE is found to be equal to 0.024 eV. For

comparison we may note that the value of ΔE is 0.04 eV for the very weak itinerant ferromagnet ZrZn_2 .²¹

We should remark that the Stoner-Wohlfarth model is highly simplified and is not able to explain other related properties of our compounds. These properties include the temperature dependence of zero field susceptibility and also a large value of electronic specific heat at low temperatures. In the Stoner-Wohlfarth model the DOS is not renormalized by the exchange interactions and so the calculation of the electronic contribution to the specific heat is not affected by exchange enhancement of the magnetic susceptibility. A satisfactory description of the zero field susceptibility and the electronic specific heat in these cases should incorporate the effects of spin fluctuation (paramagnons) on the magnetic and the thermodynamic properties at low temperatures—as discussed by Béal-Monod *et al.*²⁴ in case of a nearly ferromagnetic Fermi liquid.

DISCUSSION

The transport and magnetic measurements presented above clearly show that the metallic properties of pure CuV_2S_4 and its Zn-substituted phases undergo a qualitative change at around 90 K. Above 90 K the electronic properties are marked by the development of a pseudogap at the Fermi surface. The resistivity remains high and unsaturated. It continues to increase linearly up until the highest temperatures we have studied. In the same temperature range the thermopower has anomalous temperature dependence for a metal since it decreases linearly on heating. These are properties characteristic of a non-Fermi liquid and have been widely discussed in the literature in the context of the normal state of the high- T_c cuprates superconductors (HTS) and many heavy fermion compounds and alloys.^{18–20} In a non-Fermi liquid the notion of a quasiparticle excitation as a propagating wave packet breaks down due to the rapid decoherence of the excitation caused by strongly fluctuating interactions.²⁵ The dynamics of charge/spin becomes strongly incoherent. Below 90 K the fluctuations are suppressed in our systems and they behave like weakly correlated Fermi liquid. As a consequence resistance and thermopower decrease on cooling. In addition both χ and γ_{el} show enhancement—as expected for a nearly magnetic metal.²⁷

In its high temperature pseudogap phase the magnetic susceptibility of CuV_2S_4 shows a rapid decrease on cooling. Also in this temperature range its resistivity passes through a minimum at around 120 K. We will now present evidence that these two behaviors have a common origin and since both these properties are affected by the depletion of the DOS at the Fermi level this common origin is the existence of a pseudogap. For this we first find the residual contribution (σ_A) to the conductivity in the high temperature phase of pure CuV_2S_4 . This is calculated from the resistivity data after subtracting the linear component (BT) from the overall resistivity ($\rho_0 + A/T + BT$) and then taking the inverse (we here implicitly assume the validity of the Matthiessen's rule, i.e., the overall resistivity is the result of two alternative scattering processes and so their probabilities are additive). We then

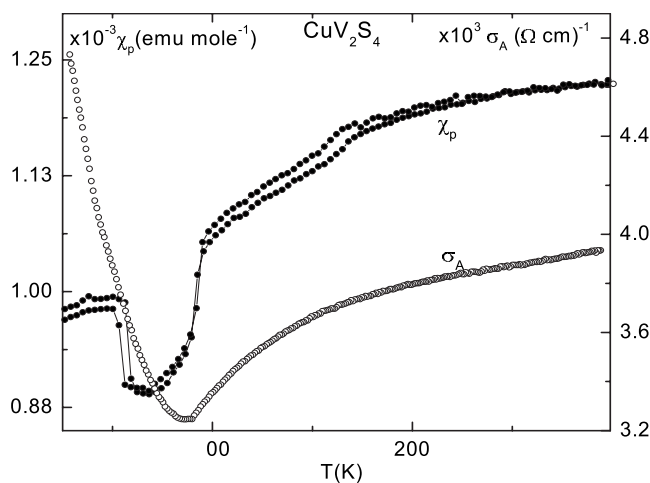


FIG. 10. The combined plot of the residual conductivity σ_A and the magnetic susceptibility χ of CuV_2S_4 . Remarkably similar patterns of decrease in σ_A and χ on cooling down to 90 K suggest their common dependence on the pseudogaplike features in DOS.

plot σ_A and χ together. As seen in Fig. 10 σ_A and χ show remarkably similar patterns of decrease on cooling down to 90 K. We interpret this correlation between the temperature dependence of σ_A and that of χ to be due to their common connection to the DOS at the Fermi level. In this sense Fig. 10 also demonstrates the evolution of the pseudogap with cooling.

Since we have mentioned the HTS and the heavy fermions as other examples of incoherent metals a few points of distinction should be noted. The CuV_2S_4 has a cubic spinel structure whereas HTS have two-dimensional anisotropic structures. HTS and the heavy fermion metals are strongly correlated electron systems. Intrinsically HTS are Mott insulators which, after the doping of holes, are driven to the boundary of metal-insulator transition. Emery and Kivelson²⁶ describe HTS as quasiparticle insulators that are rendered metallic by the localized fluctuations in the density of charge/spin of the electrons. In sharp contrast to these, CuV_2S_4 is well inside the metallic region. It has a large density of current carriers and the localization parameter of the conduction electrons is well above the Ioffe-Regel limit. This is also the reason for its properties being quite insensitive to the doping of carriers (as we have found when copper is substituted by zinc).

The electronic properties of CuV_2S_4 (including the incoherent dynamics of carriers) are intimately related to the special bonding and structural features of a pyrochlore-like lattice of V atoms. The linear chains along different $\langle 110 \rangle$ directions of the cube give rise to essentially one-dimensional bands from the d orbitals of vanadium.²⁸ This makes them unstable against the charge-ordered Peierls state. The other important feature of the network is that the anti-ferromagnetic arrangement of the spins on the V atoms is frustrated (see Fig. 1). Because of these factors the growth of charge ordering and anti-ferro correlations (of spin density) on cooling generates strong charge and spin fluctuations. (According to Matsuno *et al.*⁸ these correlated fluctuations of charges and spins along the nesting vectors $q \sim 1/4$ [110]

give rise to a pseudogap at the Fermi level of CuV_2S_4 at temperatures well above the CDW/SDW transition temperature of 90 K.) These fluctuations in turn lead to the fast decay of low energy excitations and an incoherent transport of the carriers. The breakdown of spatial homogeneity strongly renormalizes the electronic states at the Fermi level and consequently also causes the observed changes in the magnetic susceptibility, electric conductivity, and thermopower on cooling.

We will now discuss a possible mechanism that causes the enhancement of the conductivity in pure CuV_2S_4 at the lower temperatures. As discussed in the Introduction the most important aspect of the study of this compound by Fleming *et al.*⁵ was the observation of an incommensurate lattice distortion at the 90 K transition which suggested the possibility of CDW in a cubic structure. Later studies found different details of this transition and its physical origin still remains unclear. However, it is certain that there is a qualitative change in the nature of the scattering of the carriers around this temperature. A nesting model of electrons for the CDW transition is unable to explain this observation of improved conductivity in our systems (and many other layered compounds)—since a significant portion of the Fermi surface is truncated and thus the density of the carriers below the transition is reduced. However, there exists an alternative “non-nesting mechanism” for the CDW instability which was proposed by Rice and Scott.²⁹ The phenomenology of this mechanism is also applicable to the martensitic transitions observed in many well known A15 superconductors (like V_3Si , Nb_3Sn , etc.). This mechanism is more general and is able to explain the strong reduction of scattering below the transition. This model is based on the existence of saddle points on the Fermi surface. Around these points the Fermi velocity is small and the density of states is large. Thus they act as strong sinks for the electrons that are scattered in their neighborhood. On cooling the e -ph coupling across the symmetry-related saddle points causes the CDW transition and the Fermi surface is truncated only in their vicinity. The removal of the scattering sinks results in an increase in conductivity at lower temperatures. A theory applicable to CuV_2S_4 should also include the effect of inelastic e - e scattering and the pseudogap on the conductivity in its high temperature phase.

The low temperature Fermi liquid

The electronic properties of CuV_2S_4 at lower temperatures correspond to those of a weakly correlated Fermi liquid. Within the relaxation time approximation the Seebeck coefficient (S) and the specific heat coefficient (γ_{el}) can be related to the degeneracy temperature (T_F) of the Fermi liquid. This is because both these coefficients measure the entropy of the electrons. The Seebeck coefficient and the specific heat coefficient measure the transport entropy and the thermodynamic entropy of the current carriers, respectively. For a degenerate electron gas the Seebeck coefficient is given by the following expression due to Mott:¹⁵

$$S = \frac{\pi^2}{3} \left(\frac{k}{e} \right) \frac{T}{T_F} \left(\frac{\partial \ln \sigma(E)}{\partial \ln E} \right)_{E=E_F} \quad (8)$$

Here $\sigma(E)$ is the conductivity of carriers having energy E .

The value for the last term in Eq. (8) depends on the details of the scattering mechanism. It equals unity in the residual resistance region where the mean free path l is independent of energy. This is the situation we are dealing with. From the slope of the $S(T)$ curve we find the value of the Fermi temperature T_F to be between 1700 and 2200 K. These values compare quite well with the effective degeneracy temperature of around 2000 K which is found from the value of γ_{el} [$=62 \text{ mJ}/(\text{mole K}^2)$] of pure CuV_2S_4 . This agreement in the value of the parameter T_F , as estimated by these two methods, implies that the transport entropy of the current carriers in our compounds equals their thermodynamic entropy. Such equality of transport and thermodynamic entropy of the carriers in a metal is found only in exceptional cases. One such example is that of nickel near its ferromagnetic transition temperature T_C . In this case the variation of the specific heat with temperature and its divergence at T_C is found to be remarkably similar to that of the temperature derivative of the Seebeck coefficient.³⁰ According to Tang *et al.*³¹ this similarity owes its origin to the fact that Ni behaves like an “extreme itinerant-electron magnet” near its T_C . In such a situation both the transport and thermodynamic entropy of the carriers are governed by the critical fluctuations of the spin-spin correlation. This same reason may also apply to CuV_2S_4 which, at lower temperatures, behaves like Ni near its T_C , i.e., like an exchange enhanced itinerant magnet.

We have already seen that the electronic interactions in CuV_2S_4 result in a substantial enhancement of γ_{el} and χ . These interactions also affect the lifetime of the quasiparticles in a Fermi liquid and generate a Baber contribution [$\rho_{ee}(T)$] to the resistivity that is proportional to T^2 . When lattice disorder or slow spin fluctuations are present Kavesh and Wiser³² argued that an additional term, proportional to $T^{3/2}$, is also present in $\rho_{ee}(T)$. According to them $\rho_{ee}(T)$ of a Fermi liquid has the following temperature dependence:

$$\rho_{ee} = AT^2 + BT^{3/2}. \quad (9)$$

Here ρ_{ee} is obtained from the bare value by subtracting the residual resistivity at 0 K. In Fig. 11 we show the plots of ρ_{ee} versus T on a log-log scale. For both pure and Zn-substituted compounds it can be seen that ρ_{ee} varies as $T^{3/2}$ below 10 K. The Baber component seems to be absent in the resistivity of these compounds. For the Zn-substituted compounds ρ_{ee} continues to display the $T^{3/2}$ dependence up to 40–50 K. This is as expected due to the increase in the value of B in the relation (9) due to disorder. For pure samples the exponent changes to 2.4 above 10 K. At present we are unable to offer any explanation for this dependence in our pure phase.

CONCLUSIONS

We have shown that pure CuV_2S_4 and their Zn-substituted phases have non-Fermi liquidlike features in their resistivity,

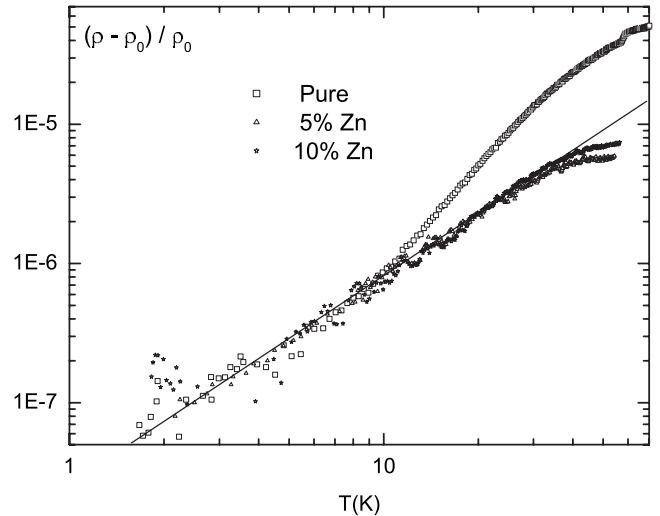


FIG. 11. The plots of $\rho_{ee} \{=(\rho - \rho_0)\}$ versus T on a log-log scale. ρ_{ee} varies as $T^{3/2}$ for both the pure and the Zn-substituted compounds below 10 K.

thermopower, and magnetic susceptibility at high temperatures. These properties have been widely discussed in the case of strongly correlated materials like high temperature superconductors and narrow band heavy fermion metals that are at the boundary of metal-insulator transition. In contrast to these our compounds are well inside the metallic region. We have argued that the rapid decay of the quasiparticles and observed incoherent metallic properties as well as a pseudogap at the Fermi level is caused by correlated fluctuations in charge/spins density of the conduction electrons in our compounds. These fluctuations result from the nearly one-dimensional nature of the d bands and the geometric frustration of the antiferromagnetic order on the pyrochlore-like network of V atoms in these compounds.

In pure CuV_2S_4 two successive transitions are observed at 90 and 55 K. The nature of these transitions is not yet clear. But there is no doubt that it is an electronic transition and below the 90 K transition the incoherent scattering is strongly suppressed. All our compounds behave as a normal and weakly correlated Fermi liquid at lower temperatures. Both the χ and γ_{el} are enhanced and the resistivity shows the expected e - e scattering contribution below 10 K. From our thermopower data we estimate the effective degeneracy temperature T_F to be in the range of 1700–2200 K. This value is consistent with our data for the specific heat γ_{el} . We have analyzed the high field magnetization data within the framework of a simple itinerant-electron model. This gives a value of 0.024 eV for the exchange splitting of d bands. It should be noted that the non-Fermi liquid effects at high temperatures have so far been observed in high temperature superconductors that happen to have layered structures. We find that our compounds also display these properties although they have cubic symmetry. This raises the question as to whether crystalline anisotropy is an essential ingredient for generating non-Fermi liquidlike features.

ACKNOWLEDGMENTS

I.N. and C.S.Y. acknowledge CSIR for financial support. The magnetic measurements were done at TIFR, Mumbai by

A. K. Nigam. The authors are grateful to A. K. Nigam, TIFR, D. Kumar, JNU, and S. Sarkar, JNU for their help, critical comments, and suggestions during this work.

¹F. K. Lotgering and R. P. van Staple, *J. Appl. Phys.* **39**, 417 (1968).
²F. J. DiSalvo and J. V. Waszczak, *Phys. Rev. B* **26**, 2501 (1982).
³M. Ito, J. Hori, H. Kurisaki, H. Okada, A. J. Perez Kuroki, N. Ogita, M. Udagawa, H. Fujii, F. Nakamura, T. Fujita, and T. Suzuki, *Phys. Rev. Lett.* **91**, 077001 (2003).
⁴(a) T. Hagino, T. Tojo, T. Atake, and S. Nagata, *Philos. Mag. B* **71**, 881 (1995). (b) P. G. Radaelli, Y. Horibe, M. J. Gutmann, H. Ishibashi, C. H. Chen, R. M. Ibberson, Y. Koyama, Y. Hor, V. Kiryukhin, and S. Cheong, *Nature (London)* **416**, 155 (2002).
⁵R. M. Fleming, F. J. DiSalvo, R. J. Cava, and J. V. Waszczak, *Phys. Rev. B* **24**, 2850 (1981).
⁶A. W. Overhauser, *Phys. Rev.* **128**, 1437 (1962).
⁷Z. W. Lu, B. M. Klein, E. Z. Kurmaev, V. M. Cherkashenko, V. R. Galakhov, S. N. Shamin, Y. M. Yarmoshenko, V. A. Trofimova, St. Uhlenbrock, M. Neumann, T. Furubayashi, T. Hagino, and S. Nagata, *Phys. Rev. B* **53**, 9626 (1996).
⁸J. Matsuno, A. Fujimori, L. F. Mattheiss, R. Endoh, and S. Nagata, *Phys. Rev. B* **64**, 115116 (2001).
⁹N. Le Nagard, A. Katty, G. Collin, and O. Gorochoy, *J. Solid State Chem.* **27**, 267 (1979), and references therein.
¹⁰D. A. Crandles, M. Reedyk, G. Wardlaw, F. S. Razavi, T. Hagino, S. Nagata, I. Shimono, and R. K. Kremer, *J. Phys.: Condens. Matter* **17**, 4813 (2005).
¹¹T. Sekine, K. Uchinokura, H. Iimura, R. Yoshizaki, and E. Matsuura, *Solid State Commun.* **51**, 187 (1984).
¹²J. Mahy, D. Colaitis, D. van Dyck, and S. J. Amelinckx, *J. Solid State Chem.* **68**, 320 (1987).
¹³Y. Yoshikawa, S. Wada, K. Miyatani, T. Tanaka, and M. Miyamoto, *Phys. Rev. B* **55**, 74 (1997); S. Wada, Y. Yoshikawa, K. Miyatani, and T. Tanaka, *J. Magn. Magn. Mater.* **177-181**, 1393 (1998).
¹⁴L. J. van der Pauw, *Philips Res. Rep.* **13**, 1 (1958).
¹⁵N. F. Mott, *Metal-Insulator Transitions* (Taylor and Francis, London, 1990); N. F. Mott and E. A. Davis, *Electronic Processes in Non-crystalline Materials* (Oxford University Press, Oxford, 1979).
¹⁶R. Horny, S. Klimm, M. Klemm, S. Ebbinghaus, G. Eickerling, and S. Horn, *J. Magn. Magn. Mater.* **272-276**, E307 (2004).
¹⁷S. J. Hagen, T. W. Jing, Z. Z. Wang, J. Horvath, and N. P. Ong, *Phys. Rev. B* **37**, 7928 (1988).
¹⁸N. Kumar and A. M. Jayannavar, *Phys. Rev. B* **45**, 5001 (1992).
¹⁹P. W. Anderson, *The Theory of Superconductivity in High-T_C Cuprates*, Princeton Series in Physics (Princeton University Press, Princeton, NJ, 1997).
²⁰G. Hildebrand, T. J. Hagenars, W. Hanke, S. Grabowski, and J. Schmalian, *Phys. Rev. B* **56**, R4317 (1997).
²¹D. M. Edwards and E. P. Wohlfarth, *Proc. R. Soc. London, Ser. A* **303**, 127 (1968).
²²A. Arrott, *Phys. Rev.* **108**, 1304 (1957).
²³M. Shimizu, *Rep. Prog. Phys.* **44**, 330 (1981).
²⁴M. T. Béal-Monod, M. A. Shang-Keng, and D. R. Fredkin, *Phys. Rev. Lett.* **20**, 929 (1968).
²⁵K. Haule, A. Rosch, J. Kroha, and P. Wölfle, *Phys. Rev. Lett.* **89**, 236402-1 (2002).
²⁶V. J. Emery and S. A. Kivelson, *Phys. Rev. Lett.* **74**, 3253 (1995).
²⁷W. F. Brinkman and T. M. Rice, *Phys. Rev. B* **2**, 4302 (1970).
²⁸D. I. Khomskii and T. Mizokawa, *Phys. Rev. Lett.* **94**, 156402 (2005).
²⁹T. M. Rice and G. K. Scott, *Phys. Rev. Lett.* **35**, 120 (1975).
³⁰F. J. Blatt, P. A. Schroeder, C. L. Foiles, and D. Greig, *Thermoelectric Power of Metals* (Plenum Press, New York, 1976).
³¹S. H. Tang, P. P. Craig, and T. A. Kitchens, *Phys. Rev. Lett.* **27**, 593 (1971).
³²M. Kavesh and N. Wiser, *Adv. Phys.* **33**, 257 (1984).